Author Manuscript

Author Manuscript

Author Manuscript

Author Manuscript

HHS Public Access

Author manuscript

Clin Cancer Res. Author manuscript; available in PMC 2023 June 01.

Published in final edited form as:

Clin Cancer Res. 2021 December 15; 27(24): 6726–6736. doi:10.1158/1078-0432.CCR-21-1650.

Phase Ib/II Study of Cetuximab plus Pembrolizumab in Patients with Advanced RAS Wild-Type Colorectal Cancer

Christos Fountzilas[1], **David L. Bajor**[2], **Sarbajit Mukherjee**[1], **Joel Saltzman**[2], **Agnieszka K. Witkiewicz**[1], **Orla Maguire**[1], **Hans Minderman**[1], **Ram Nambiar**[1], **Hanna R. Rosenheck**[1], **Erik S. Knudsen**[1], **Jason B. Muhitch**[1], **Scott I. Abrams**[1], **Chong Wang**[1], **Alan D. Hutson**[1], **Kristopher Attwood**[1], **Karen A. Hicks**[1], **Jennifer A. Jurcevic**[1], **Pawel Kalinski**[1], **Renuka Iyer**[1], **Patrick M. Boland**[3]

[1]Roswell Park Comprehensive Cancer Center, Buffalo, New York

[2]Case Comprehensive Cancer Center, Cleveland, Ohio

[3]Rutgers Cancer Institute of New Jersey, New Brunswick, New Jersey.

Abstract

Purpose: We evaluated the antitumor efficacy of cetuximab in combination with pembrolizumab in patients with *RAS* wild-type (RASwt), metastatic colorectal adenocarcinoma (mCRC).

Experimental Design: In this phase Ib/II study, cetuximab was combined with pembrolizumab in patients with RASwt mCRC with ≥ one prior line of therapy for advanced disease. We analyzed baseline on-treatment tumor tissues for changes in the tumor microenvironment (TME), using flow cytometry and multispectral immunofluorescence.

Results: Forty-four patients were evaluable for efficacy. The study was negative for the primary efficacy endpoint (overall response rate: 2.6%, 6-month progression-free survival: 31%; p=0.52). Median PFS was 4.1 months (95% CI: 3.9–5.5 months). No increase in adverse effects was identified. We observed favorable immunomodulation with 47% increase in the number of intratumoral cytotoxic T-cell lymphocytes post-treatment (p=0.035). These changes were more pronounced in patients with tumor shrinkage (p=0.05). The TME was characterized by high numbers of $TIM3^+$ and $CTLA4^+$ cells; there were few activated $OX40^+$ cells. PD-L1 expression was higher in pre-treatment tumor cells from metastatic sites vs. primary tumor samples ($p<0.05$). Higher numbers of $PD\text{-}L1^+$ tumor cells at baseline were associated with tumor shrinkage (p=0.04). Analysis of immune populations in the blood demonstrated decreases in $PD\text{-}1^+$ memory effector cells (p=0.04) and granulocytic MDSCs (p=0.03), with simultaneous increases in $CD4^+/CTLA4^+$ cells (p=0.01).

Conclusions: The combination of cetuximab and pembrolizumab is inactive in patients with RASwt mCRC, despite its partial local immunologic efficacy. Further development of immuno-

Corresponding Author: Christos Fountzilas MD, Department of Medicine/Division of Gastrointestinal Medicine and Early Phase Clinical Trial Program, Roswell Park Comprehensive Cancer Center, Elm & Carlton St, Buffalo NY, 14263. Phone: 716-845-8974. Christos.Fountzilas@RoswellPark.org. Fax: 716-845-8935.

Conflict of Interest Disclosure Statement: Christos Fountzilas has research support for this study from Merck Sharp & Dohme Corp (paid to the institute). The other authors report no relevant disclosures.

Author Manuscript Author Manuscript Author Manuscript Author Manuscript

oncology combinations with enhanced efficacy and/or targeting additional or alternative immune checkpoints merits investigation.

Keywords

Cetuximab; Pembrolizumab; Colorectal Cancer; Tumor Microenvironment

Introduction

Colorectal cancer (CRC) is the 3rd most common cancer in the United States (1). Patients with advanced disease have a dismal prognosis and, despite recent progress, the 5-year overall survival (OS) remains less than 15% (2). Forty to 60% of all CRC cases harbor activating mutations in *K-RAS* and *N-RAS* genes (3–5), a negative predictive biomarker for clinical benefit from monoclonal antibodies (mAbs) targeting the epidermal growth factor receptor (EGFR) such as cetuximab and panitumumab (6–9). Cetuximab and panitumumab are commonly used in patients with *RAS* wild-type (RASwt) and *BRAF* wild-type (BRAFwt) CRC, either as single agents or, more commonly, in combination with chemotherapy (10). Despite high initial response rates, resistance and progression inevitably develops within months from initiation of treatment.

The mechanism of action of EGFR-targeting mAbs involves both inhibition of the EGFR-RAS-MAPK axis as well as antigen-dependent cell cytotoxicity (ADCC) mediated via $CD3^{-}CD16^{+}CD56^{+}$ natural killer (NK) cells (11,12), the later potentially unrelated to the RAS mutational status of the tumor (13). In retrospective studies, the addition of anti-EGFR mAbs to chemotherapy is associated with increased density of cytotoxic CD8+ (CTLs), effector memory (CD45RO+) and regulatory (FOXP3+) T-cells within metastases as compared to no treatment, chemotherapy alone or chemotherapy plus anti-VEGF mAbs (14). Further, the anti-EGFR plus chemotherapy combination is associated with increased densities of cells expressing the inhibitory immune checkpoint, programmed death-1 (PD-1). Activation of NK cells by cetuximab induces PD-1 expression; inhibition of PD-1 increases cetuximab-induced NK cell activation and cytotoxicity against tumor cells expressing the PD-ligand 1 (PD-L1) (15). In patients with squamous cell carcinoma of the head and neck, though cetuximab and panitumumab both inhibited EGFR to the same extent, cetuximab led to increased dendritic cell (DC) maturation and antigen cross-presentation to CTLs and increase in EGFR-specific CTLs, perhaps related to its IgG1 specificity (16). In patients with advanced CRC, treatment with cetuximab increased intratumoral CTLs and expression of inhibitory immune checkpoints including the PD-1/PD-L1 axis (17). In addition, in a syngeneic mouse CRC model (CT-26 cell line), combined MAPK pathway and PD-1 inhibition was shown to be of benefit, where PD-1 provided little benefit on its own (18).

We hypothesized that a therapeutic strategy jointly targeting the EGFR-RAS-MAPK pathway and the critical immune checkpoint, PD-1, would enhance intratumoral T-cell infiltration and consequently improve clinical outcomes for patients with metastatic, RASwt CRC. To test this hypothesis, we designed a phase Ib/lI study of cetuximab plus pembrolizumab, a blocking mAb targeting PD-1. Here, we present the clinical outcomes and correlative studies of this trial. Though the clinical efficacy of this regimen was suboptimal,

Author Manuscript Author Manuscript Author Manuscript Author Manuscript

we noted favorable immunomodulatory changes in both tumor and peripheral blood. Further, our correlative studies provide insight into potential immunologic resistance mechanisms and informs future development of chemotherapy-free approaches combining anti-EGFR mAbs and immune checkpoint inhibitors in RASwt CRC.

Materials and Methods

Study Design

This was a multi-institutional single-arm phase Ib\II study of cetuximab in combination with pembrolizumab in patients with metastatic, RASwt CRC who were eligible for anti-EGFR therapy (i.e., anti-EGFR therapy naïve or appropriate for anti-EGFR rechallenge). The study included an initial phase Ib, lead-in safety cohort. Safety was established with the enrollment of 9 patients (with 6 completing at least two cycles of study treatment), and the phase II part was initiated.

The study was approved by the Institutional Review Board (IRB) in all participating institutions (Roswell Park Comprehensive Cancer Center and Case Comprehensive Cancer Center), conducted in accordance with the Declaration of Helsinki and registered at clinicaltrials.gov (NCT02713373). Written informed consent was obtained from each subject or each subject's guardian.

Patient Population

We enrolled adult patients with pathologically confirmed metastatic, RASwt (defined as wild-type for both KRAS and NRAS) CRC who had received at least 1 prior systemic therapy in the metastatic or unresectable disease setting. Patients with BRAF mutation and microsatellite instability high/mismatch repair deficient (MSI-H/dMMR) CRC were allowed to participate. Eligible patients were appropriate for anti-EGFR therapy, defined as naive to anti-EGFR therapy (cetuximab or panitumumab) or a candidate for rechallenge by virtue of the following: a) the investigator deems anti-EGFR retreatment with cetuximab to be a reasonable standard of care option AND b) the outcome of prior anti-EGFR therapy was not rapid progression (defined as 3 or less months on therapy) AND c) prior anti-EGFR therapy was administered > 6 months prior to the start of study therapy. Patients had Eastern Cooperative Oncology Group (ECOG) performance status (PS) of 0–2, preserved bone marrow, liver and kidney function, and measurable disease per RECIST 1.1 criteria. Patients with active autoimmune disease in the past 2 years, history of non-infectious pneumonitis, immunodeficiency syndrome or immunosuppressive therapy, or prior severe infusion reaction to cetuximab where excluded. Eligible patients should also provide fresh tumor tissue for correlative studies; archived tissue was accepted for those patients whose biopsy was not safe or feasible.

Treatment and Procedures

A cycle was defined as 3 weeks of treatment, with cetuximab administered weekly and pembrolizumab administered every 3 weeks, on day 1 of each cycle. Cetuximab 400 mg/m2 loading dose was administered on Cycle 1 Day 1, followed by 250 mg/m^2 intravenously (IV) weekly (see Study Schema, Figure 1A). Pembrolizumab 200 mg was administered as a

Author Manuscript Author Manuscript Author Manuscript Author Manuscript

fixed dose IV every 3 weeks. In the absence of relevant limiting toxicities, pembrolizumab could be administered even if cetuximab was held for cetuximab-related adverse events (AEs). Likewise, in the instance of pembrolizumab related AEs which require dose holding or discontinuation, cetuximab administration could continue as appropriate. Cetuximab was administered prior to pembrolizumab on Day 1, due to concern for infusion reactions. Pembrolizumab administration on Day 2 of any cycle was permitted in the event of a cetuximab infusion-related reaction (IRR) or any other AE at the discretion of the investigator. If cetuximab was held for more than 2 weeks for reasons other than cetuximab-related AEs, the 400 mg/m^2 loading dose could be readministered upon resumption, at the discretion of the investigator. Response evaluation using cross-sectional imaging was performed every 9 weeks. Tumor biopsy was performed at baseline (up to 30 days prior to initiation of treatment on Day 1) and optionally before Cycle 4. Either the primary or a metastasis could be biopsied. Baseline archival tissue samples were accepted where a biopsy was not feasible or posed excess risk. Blood samples for correlative studies were collected at baseline, and prior to Cycles 2 and 4.

Study Objectives and Endpoints

The primary objective was to determine the clinical efficacy of the cetuximab plus pembrolizumab combinations in patients with RASwt, metastatic CRC who were eligible for anti-EGFR therapy. We used the objective response rate (ORR) by RECIST 1.1 and 6-month progression-free survival (PFS) as co-primary endpoints for efficacy. Secondary objectives included determination of safety of the combination and OS. The identification of biomarkers of response and/resistance to therapy in the tumor and peripheral blood was an exploratory endpoint.

Flow Cytometry

Peripheral blood and tumor tissue were collected in sodium heparin tubes and cold RPMI in accordance with the IRB-approved protocol, respectively. Single cell suspensions were generated from tumor biopsies by mechanical digestion using a Medimachine (BD Biosciences, San Jose, CA) using a 70 μm filter. Once washed, cells were immunophenotyped in cold FCM Buffer (1x PBS + 0.5% BSA). Cells were immunophenotyped using three panels for flow cytometry. All antibodies were mouse monoclonal antibodies. Since cellularity of tumor biopsies was not consistent, a panel priority was set (1–3) which meant that not all panels were run for all tumor biopsies. Panel 1 included CD45 (BD Biosciences, clone 2D1), CD3 (Beckman Coulter, clone UCHT1), CD8 (BD Biosciences, clone HIT8a), CD45RO (BD Biosciences, clone UCHL1), CD16 (BD Biosciences, clone CLB), CD56 (BD Biosciences, clone NCAM16.2), CD14 (BD Biosciences, clone MΦP9), PD-1 (Biolegend, clone 29E.2A3), PD-L1 (BD Biosciences, clone MIH4). Panel 2 included CD45 (2D1), Lineage (CD3, CD19 BD Biosciences, clone HIB19, CD56), HLA-DR (ThermoFisher, clone TU36), CD33 (Beckman Coulter, clone D3HL60.251), CD11b (Beckman Coulter, clone Bear1). Panel 3 included CD45 (2D1), CD3 (UCHT1), CD4 (BD Biosciences, clone RPA-T4), FoxP3 (Biolegend, clone 206D), GARP (BD Biosciences, clone 7B11), CTLA4 (BD Biosciences, clone BNI3). Following staining for surface markers, tumor cells were washed with cold FCM buffer. Red blood cells were lysed in peripheral blood samples using Ack Lysing buffer (ThermoFisher, Grand Island,

Author Manuscript Author Manuscript Author Manuscript Author Manuscript

NY) and cells were washed with cold FCM buffer. Panel 3 contained intracellular FoxP3 and CTLA4, so following wash, cells were stained for FoxP3 and CTLA4 using Foxp3/ Transcription Factor Staining Buffer Set (ThermoFisher). Flow cytometry acquisition and compensation was performed on an LSR Fortessa (BD Biosciences, San Jose, CA, USA). Analysis of listmode data was performed using Winlist 8.0 (Verity Software House, Inc., Topsham, ME, USA).

Multispectral Immunofluorescence Staining (MIF)

Tumor samples were fixed in formalin and embedded in paraffin (FFPE) and 4 μm thick sections were cut for staining. A pathologist (AW) evaluated hematoxylin and eosin (H&E) stained slides from each FFPE block. MIF staining was performed on the BOND RX^{m} Research Stainer (Leica Biosystems). The MIF panel consisted of the following antibodies (clone, company, and opal fluorophores): TIM3 (D5D5R™, Cell Signaling, Opal 540), CTLA4 (UMAB249, Biocare Medical, Opal 570), OX40 (E9U7O, Cell Signaling, Opal 520), PD-L1 (E1L3N, Cell Signaling, Opal 620), LAG3 (D2G4O, Cell Signaling, Opal 650), pancytokeratin (AE1AE3, Agilent DAKO, Opal 690). All AKOYA reagents used for MIF staining are part of a detection kit (NEL821001KT). Spectral DAPI (AKOYA Biosciences) was applied once slides were removed from the BOND. They were cover slipped using an aqueous method and Diamond antifade mounting medium (Invitrogen, ThermoFisher). Slides were imaged on the Vectra® Polaris Automated Quantitative Pathology Imaging System (AKOYA Biosciences). Spectral unmixing, tissue and cell segmentation, and cell phenotyping were performed on inForm® Software v2.4.8 (AKOYA Biosciences).

Statistical Analysis

We utilized two co-primary efficacy endpoints for this study, the proportion of patients achieving complete or partial RECIST objective response and the proportion surviving progression-free for at least six months; we would declare the combination worthy of further investigation if it showed activity on either endpoint. We utilized a single-stage version of the bivariate design described by Sill et al (19). Based on historical data, the ORR for cetuximab alone in this patient population is approximately 20%, and the proportion of patients surviving progression-free for at least six months is approximately 30% (20). We set the following null (ORR H0=20%, 6-month PFS H0=30%) and alternative hypotheses (ORR H1=40%, 6-month PFS H1=50%) indicating inactivity or activity for the two endpoints, respectively. Assuming independence of the two endpoints, we targeted 42 eligible and treated patients, requiring at least 38 eligible and treated in order to have ≥80% power to detect activity based on response alone, ≥80% power to detect activity based on 6-month PFS alone, and ≥97% power if the regimen is active on both endpoints. Type I error was controlled at <0.10. The exact binomial test was used to compare the ORR and 6-month PFS percentages. The correlative analysis was exploratory in nature and no adjustments for multiple testing were made. All tests about the correlation rho=0 were tested at level alpha=0.05.

Funding Source

The study was funded by a grant provided by Merck Sharp & Dohme Corp who also provided pembrolizumab free of charge.

Author Manuscript Author Manuscript Author Manuscript Author Manuscript

Data Availability Statement

The data generated in this study are available upon request from the corresponding author.

Results

Study Population

Forty-five patients were enrolled; one patient was not treated secondary to clinical progression during screening (Supplementary Figure 1). We initially enrolled 9 patients onto the phase Ib part of the study from August 10th, 2016 to November 2nd, 2016. No DLTs were observed and accrual continued until October 22nd, 2019. Forty-four patients received at least one dose of study treatment. Two subjects withdrew consent for IRR following one dose of study therapy and were replaced. The median age of the 44 treated patients was 64 years (range 34–80), 68% were male and 73% had a left-sided primary tumor. Most patients (93%) had no prior therapy with anti-EGFR mAb. The patients baseline demographics are presented in Table 1.

Antitumor Efficacy

At the time of data cut off (December 29th 2020), all patients were off study treatment. The most common reason for treatment discontinuation was disease progression (82%; see Supplementary Figure 1). One patient (left-sided, mismatch repair proficient [pMMR]/BRAFwt tumor) attained a partial response (PR) for an ORR of 2.6% (Figure 1B). Sixty-nine percent of the patients had stable disease (SD) as best response. The median PFS was 4.1 months (95% CI: 3.9–5.5 months) for a 6-month PFS rate of 31% (95% CI: 20–43%) (Figure 1C). The overall p-value for the joint test of efficacy was p=0.52. As such the study was negative for the primary endpoint of efficacy. The median OS was 14.5 months (95% CI: 11.8–19.9 months) (Figure 1D). Of the 39 patients evaluable for response, 17 (44%) patients showed a decrease in size of target lesions (Figure 1B). Six patients had decrease in size of target lesions between 20–29%; four with left-sided primary and 2 with right-sided primary. Eighteen percent of the patients had decrease in CEA >50% (Supplementary Figure 2). Of the three anti-EGFR mAb pre-treated patients (all pMMR), two (rectal and cecum primary) had SD and 1 (rectal primary) had progressive disease (PD) as best response. The patient with rectal primary and SD had tumor shrinkage by RECIST 1.1. None had significant biochemical response. Their PFS and OS ranged between 2–6 months and 9.8–17.7 months, respectively.

Safety

Forty-three patients experienced at least one AE (Supplementary Table 1). The most common AEs were dry skin (n=21), acneiform dermatitis (n=20), fatigue (n=17), hypomagnesemia (n=17), rash (n=16), diarrhea (n=13), pruritus (n=13), and anorexia (n=10) (Supplemental Table 1). The AEs were mainly grade 1 or 2, the most common grade 3 or 4 AEs were hypomagnesemia (n=4) and acneiform rash (n=2). AEs of special interest included IRR (n=9, grade 1/2: 8, grade 3: 1), transaminase elevation (n=8, grade 1/2:6 grade 3: 2), hypo- or hyperthyroidism (n=4, all grade 1 or 2); there was one patient with grade 2

Author Manuscript Author Manuscript Author Manuscript Author Manuscript

pneumonitis and one with grade 3 pancreatitis. There was one patient who developed grade 1 bullous dermatitis. No indication for enhanced toxicity of the tested combination was seen.

Intratumoral CTLs are increased with combination therapy

We performed flow cytometry in fresh tumor tissue at baseline and before Cycle 4 (Figure 2A–B). Sixteen patients had paired fresh tumor samples appropriate for flow cytometry. Post-treatment biopsies showed a 47% increase in the numbers of tumor-infiltrating CTLs ($CD3^+/CD8^+$; p=0.035). Both exhausted PD-1^+ CTLs and exhausted PD-1^+ memory effector T-cells ($CD3^+/CD8^+/CD45RO^+$) decreased by 23% but neither reached statistical significance. An increase in NK cells ($CD3^-/CD16^+/CD56^+$) by 113% was observed, though this did not reach statistical significance (p=0.3). No significant changes were noted in other intratumoral lymphoid cells including T_{regs}, possibly due to a small sample size.

We then attempted to correlate baseline and on-treatment changes in intratumoral immune cells with clinical endpoints (Supplementary Table 2A). We considered any decrease in tumor size, significant decrease in CEA (>50%), prolonged disease control (defined as PFS>6 months) and survival (defined as OS>12 months) as clinically meaningful positive outcomes. We did not identify any baseline immune cell population that was significantly associated with any of the above positive outcomes. There was a trend for higher baseline NK cells in patients with any level of tumor shrinkage and decrease in CEA >50% compared to patients without (29% and 29% vs. 14% and 17% respectively, Supplementary Figure 3).

Patients with any decrease in tumor size showed intratumoral CTLs increase by 96% (vs. 36% in patients with no change or increase in size, p=0.05; Figure 3A) on-treatment. Similarly, in patients with CEA decrease >50%, intratumoral CTLs increased by 96% vs 39% in patients without (p=0.035; Figure 3B). Memory $CD8^+$ T-cells decreased by 26% in patients with CEA decrease >50% (vs. increase by 5% in patients without, p=0.05). There was no significant association between any positive clinical outcome and intratumoral NK cell changes on-treatment, though there was a trend for higher percentage increase in NK cells in patients with PFS>6 months and OS>12 months. In contrast, there was a trend toward decrease in NK cells among patients with tumor shrinkage as well as CEA decrease >50% vs. not, though not reaching significance. The seemingly contradictory results may be related to increased apoptosis of exhausted NK cells in patients with higher degrees of tumor shrinkage.

The RASwt CRC tumor microenvironment (TME) is characterized by low PD-L1 and high TIM3 and CTLA4 expression

MIF was performed for PD-L1 and other T-cell exhaustion markers (TIM3, CTLA4, LAG3), as well as activation marker OX40. Cells were defined as: partially activated-1 ($OX40^+/AE1\_AE3^-/PD\text{-}L1^-$, positive for 1/3 exhaustion markers), partially activated-2 ($OX40^+/AE1\_AE3^-/PD\text{-}L1^-$, positive for 2/3 exhaustion markers), partially activated-3 ($OX40^+/AE1\_AE3^-/PD\text{-}L1^-$, positive for 3/3 exhaustion markers), exhausted-1 ($OX40^-/AE1\_AE3^-/PD\text{-}L1^-$, positive for 1/3 exhaustion markers), exhausted-2 ($OX40^-/AE1\_AE3^-/PD\text{-}L1^-$, 2/3 positive for exhaustion markers), and exhausted-3 ($OX40^-/AE1\_AE3^-/PD\text{-}L1^-$, positive for 3/3 exhaustion markers). We observed that the TME in

Author Manuscript Author Manuscript Author Manuscript Author Manuscript

advanced, RASwt CRC is characterized by high numbers of cells with expression of at least one marker of exhaustion beyond PD-L1 (Figure 4A–F). Indeed, the TME was characterized by high numbers of $TIM3^+$ and $CTLA4^+$ cells, while $PD\text{-}L1^+$, $LAG3^+$ and $OX40^+$ cells were relatively few (Supplementary Figure 4A, Supplementary Table 2B). Expression of PD-L1 was higher in tumor cells in pre-treatment samples from metastatic sites vs. primary tumor samples ($p<0.05$; Figure 4A, Supplementary Figure 4B). On the contrary, pre-treatment specimens from the primary tumors had more activated (i.e., $OX40^+/AE1\_AE3^-$ cells without expression of any exhaustion markers), partially activated-1 and exhausted-1 cells compared to specimen from metastatic sites ($p<0.001$; Figure 4E–F, Supplementary Figure 4B).

Overall, we noted a trend for increased numbers of activated and partially activated-1 cells and decreased $PD\text{-}L1^+$ tumor cells in response to treatment, but there was no change in the number of $PD\text{-}L1^-$ cells expressing other exhaustion markers (Supplementary Table 2B, Supplementary Figure 4C). Increased numbers of $PD\text{-}L1^+$ tumor cells at baseline were associated with decreases in tumor size on treatment ($p=0.04$; Figure 3C, Supplementary Table 2C). The only patient with PR (RP-01–32) had high TIM3, intermediate OX40 and PD-L1, and low LAG3 and CTLA4 expressions (Figure 3D). Interestingly, the number of activated cells at baseline was lower in patients with PFS of 6 months of more, probably related to the overall sparsity of activated cells ($p=0.03$; Supplementary Figure 4D, Supplementary Table 2C). In patients with CEA decrease >50%, the number of activated T-cells and partially activated-1 cells decreased on treatment by 88% and 100% respectively (vs. 29% increase and 22% decrease in patients without respectively, $p=0.03$; Supplementary Figure 4E, Supplementary Table 2C). Again, the number of these cells was small in analyzed specimens. It is also plausible that the association of decrease in their numbers on treatment with favorable outcome may be related to increased antitumor activity subsequently leading to phenotypic conversion to exhausted cells.

$CTLA4^+$ T_{regs} in peripheral blood increased on treatment

We performed flow cytometry in peripheral blood samples at baseline and on treatment (Supplementary Table 2D). Changes of immune cell populations in peripheral blood over time are depicted in Supplementary Figure 5. The $PD\text{-}1^+$ memory effector T-cells decreased by 42% ($p=0.05$) and granulocytic myeloid-derived suppressor cells (gMDSCs) by 30% ($p=0.03$) by cycle 4. In contrast, $CTLA4^+/CD4^+$ T-cells increased by 37% ($p=0.01$) over the same time period. $CTLA4^+$ Tregs increased by 16% ($p=0.06$). Non-significant changes were seen in multiple additional peripheral blood populations, as described next. A decrease in CTLs by 5% and $PD\text{-}1^+$ exhausted $CD8^+$ T-cells by 48% was favored. NK cells trended toward decrease by 15% on treatment. Finally, the T_{eff}/T_{reg} ratio increased by 30% by cycle 4, also not reaching statistical significance.

We then evaluated how the baseline status of different immune cell populations and changes on treatment correlate with positive clinical outcomes (Supplementary Table 2E). Patients with PFS>6 months had lower numbers of CTLs in peripheral blood at baseline ($p=0.04$) while patients with decrease in tumor burden had higher numbers of exhausted $PD\text{-}1^+$ $CD8^+$ T-cells and exhausted $PD\text{-}1^+$ $CD8^+$ $CD45RO^-$ T-cells ($p=0.04$ and 0.02 respectively). The

Author Manuscript Author Manuscript Author Manuscript Author Manuscript

number of T_{regs} at baseline in patients with decrease in CEA>50% was slightly higher compared to patients without (p=0.03).

In terms of on-treatment dynamics, PD-1^+/$CD8^+$/$CD45RO^-$ T-cells decreased by 82% and 78% by cycle 4 in patients with PFS>6 months and OS>12 months respectively (vs. 8% decrease and 278% increase, p=0.03). Similarly, PD-1^+/$CD8^+$/$CD45RO^-$ T-cells decreased by 78% in patients with decrease in tumor burden vs. 17% but this did not reach statistical significance (p=0.07). Patients with OS>12 months had 61% decrease in $CD4^+$ $GARP^+$ T-cells vs. 21% increase in patients with OS<12 months (p=0.03). Patients with decrease in CEA>50% had 43% decrease in T_{regs} by cycle 4 vs. 50% increase in patients without (p=0.03). Similarly, the T_{eff}/T_{reg} ratio decreased by 43% in this patient population (vs. 37% increase, p=0.04).

Outcomes in Patients with Mismatch Repair Deficient or BRAF mutated tumors

Pembrolizumab has evolved as an active treatment option in patients with advanced, MSI-H/dMMR CRC regardless of the RAS or BRAF status (21,22). Overall, 4 patients with dMMR or MSI-H tumors were enrolled. Three patients (RP-01–09, RP-01–06, and RP-01–04) had dMMR tumors; one, RP-01–23, had a pMMR tumor, with the PCR assay demonstrating MSI-H status. Prior exposure to immune checkpoint inhibitors, clinical outcomes and immune checkpoint status by MIF for the MSI-H/dMMR patients are summarized in Figure 5A. The progression-free time for the 3 patients with SD ranged between 4–6 months. All patients had low OX40 expression. Patient RP-01–23, who attained a near PR with deep CEA response, had low expression of all negative immune checkpoints except for TIM3 (Figure 5B). On the contrary, the only patient with PD as best response had high TIM3, CTLA4 and PD-L1 expression (Figure 5C).

Two patients had BRAF V600-mutant/pMMR tumors. Both had SD as best response with progression-free time of 4 (LH-01–26) and 9.4 (UH-01–31) months. The first had 3% decrease in tumor burden and the second 14% increase. The baseline values of CTLs (62.42), PD-1^+ exhausted CTLs (75.65), effector memory T-cells (89.79) and PD-1^+ exhausted memory T-cells (80.47) for patient LH-01–26 were all above the overall study population median (Supplementary Table 3). No baseline fresh tissue was available for patient UH-01–31.

Discussion

EGFR-targeting mAbs have improved outcomes when used in combination with cytotoxic therapy in patients with RASwt mCRC (6–8). Anti-EGFR monotherapy remains a therapeutic option, though with slightly lesser activity and most often used in later lines of therapy (20). In this phase Ib/II study, we attempted to improve the antitumor efficacy of cetuximab by the addition of the PD-1 inhibitor pembrolizumab. Despite the improvements in the TME observed in our study, the combination of cetuximab and pembrolizumab failed to improve ORR or PFS compared to cetuximab alone. The PFS and OS results appear similar to that observed with EGFR monotherapy strategies, though the ORR would seem to be lower (20). Thus, the strategy of combined PD-1 and EGFR inhibition cannot be recommended for further development in unselected patients with RASwt CRC.

Author Manuscript Author Manuscript Author Manuscript Author Manuscript

In the recently reported phase II CAVE study, cetuximab was combined with the PD-L1 mAb avelumab in patients with RASwt CRC who had achieved prior response (CR or PR) to 1st-line chemotherapy plus an anti-EGFR mAb and subsequently received a 2nd-line systemic therapy (23). While the ORR appears higher in CAVE compared to our study (7% vs 2.6%), the PFS and OS appear similar, if not slightly superior in our study (6-month PFS 31% vs 20%, and 12-month OS 60% vs. 50%). Cross trial comparisons are difficult mainly because patients in CAVE were preselected based on prior favorable response to anti-EGFR mAb vs. a predominantly (93%) anti-EGFR mAb-naïve patient population. In addition, inherent tumor heterogeneity and presence or emergence of cetuximab-resistant clones may have negatively affected outcomes. Patients with detectable RAS mutations in ctDNA at baseline in the ASPECCT study had worse OS compared to patients with undetectable mutations, while identification of RAS mutations while on treatment with anti-EGFR therapy was not (24). Presence of RAS/BRAF mutations in ctDNA in CAVE (27% of patients) predicted for worse short- and long-term oncologic outcomes. The percentage of ctDNA-detected baseline and treatment-emergent RAS and BRAF mutations is unknown in our study. Parseghian et al recently reported the prevalence of acquired resistance mutations (RAS, BRAF, EGFR, and MAP2K1) in ctDNA in patients treated in 1st- vs. 3rd-line setting (25). The incidence of resistance mutation acquisition was less than 10% in patients treated with chemotherapy plus anti-EGFR mAb in 1st-line and was similar to patients who were treated with chemotherapy alone (7.5 vs 6.8%, p=1). At the same time, 45% of patients treated in 3rd-line acquired EGFR resistance mutations. Though the correlative studies in our study were designed to primarily answer immunology questions, we are planning further correlative genomic studies using blood and tumor tissue specimens to dissect resistance to treatment.

In localized CRC, increased densities of tumor-infiltrating CTLs and effector memory $CD8^+$ T-cells in the TME are associated with decreased invasion and improved long-term outcomes (26–28). Overall densities of tumor-infiltrating lymphocytes are lesser in microsatellite stable/low tumors, as compared to MSI-H tumors, potentially representing one of the factors contributing to their differential responsiveness to immune checkpoint inhibitors. In past investigations, increased densities of CTLs at baseline associated with benefit from PD-(L)1 blockade (29). Thus, we hypothesized 1) that the addition of cetuximab to pembrolizumab would increase CTLs within the TME and 2) that this TME modulation would convert PD-1 resistant tumors to PD-1 sensitive tumors. Consistent with our hypothesis, we observed favorable immune changes within the TME, including significant increases in intratumoral CTLs (47% overall, and 96% in cases with tumor shrinkage), as well as a trend toward increased NK cells (113%). Additional significant findings were that exhausted $PD\text{-}1^+$ T-cells and gMDSCs decreased in peripheral blood. We speculate that the associated decrease in CTLs in peripheral blood reflect their re-direction into the tumors. That the increase in intratumoral CTLs is most pronounced in patients with decrease in tumor size and significant biochemical response is in line with the mechanism of action of both cetuximab and pembrolizumab. However, the lack of improved clinical outcomes suggests inactivity of pembrolizumab despite this TME modulation, potentially related to a yet inadequate degree of intratumoral T-cell trafficking and survival in tumors that are ‘cold’ at baseline. On the other hand, it is possible that the CTL infiltration observed may largely represent

Author Manuscript Author Manuscript Author Manuscript Author Manuscript

an inflammatory, but non-tumor directed CTL population. Further studies sequencing the T-cell receptors in available specimens may provide significant insight. Finally, the impact of additional inhibitory cellular populations and signaling pathways remains a potential contributor of major concern. For consideration in future investigation, we observed striking TME differences between the primary and metastatic tumor sites. Our data indicate that analysis of the primary tumors may not adequately reflect the immunosuppressive status of the metastatic sites.

Several findings from our correlative studies may provide additional insight into the reasons this combination had suboptimal performance. When present at baseline, high PD-L1 expression predicted for decrease in tumor size with cetuximab/pembrolizumab. Higher numbers of exhausted PD-1^+/$CD8^+$ and PD-1^+/$CD8^+$/$CD45RO^-$ T-cells in peripheral blood at baseline correlated with decrease in tumor burden while PD-1^+/$CD8^+$/$CD45RO^-$ T-cells decreased significantly on treatment in patients with PFS>6 months and OS>12 months. However, MIF revealed that intratumoral PD-L1 expression was uncommon. The main inhibitory immune checkpoints expressed in these tumors were TIM3 and CTLA-4. Supporting a contributory role of alternative immune checkpoints, we noted an increase in $CTLA4^+$ $CD4^+$ T-cells and $CTLA4^+$ T_{regs} in the peripheral blood during treatment. Interestingly, another study recently reported preliminary results utilizing the combination of panitumumab with the PD-1 inhibitor nivolumab and the CTLA-4 inhibitor ipilimumab in RASwt/BRAFwt mCRC patients (30). The triplet regimen produced an ORR of 35%, median PFS of 5.7 months and median OS of 27 months (30). Thus, the anti-EGFR/PD-1/CTLA4 combination would appear to be more active compared to dual anti-EGFR and PD-(L)1. This raises a possibility that targeting additional exhaustion or activation pathways may improve the efficacy of novel chemotherapy-free, immuno-oncology approaches in mCRC.

Pembrolizumab is active in patients with MSI-H/dMMR CRC with prior exposure to chemotherapy (22). Despite this, a considerable fraction of patients with MSI-H/dMMR tumors do not benefit from PD-1 monotherapy. We did not observe a significant antitumor effect with cetuximab/pembrolizumab in dMMR/MSI-H tumors, though 2/4 patients had previously progressed on PD-1 monotherapy. While a negative impact of incorporation of anti-EGFR mAb in patients with MSI-H/dMMR and RASwt CRC cannot be excluded (31), we did notice high CTLA4 expression in the only patient who had PD while it was low in the only patient who had a near PR. Combinations of anti-CTLA4 plus anti-PD-1 mAbs are active in MSI-H/dMMR CRC with ORR that appears higher compared to anti-PD-1 monotherapy at the expense of higher toxicity (32,33). Interestingly, the tumor RAS status may be predictive of the benefit from anti-PD-1 monotherapy in MSI-H/dMMR CRC but not from anti-PD-1/CTLA4 combinations (32,34).

Finally, BRAF V600-mutated CRC is an aggressive molecular subtype of CRC with poor outcomes on 2^{nd}-line cytotoxic therapy as well as resistance to anti-EGFR mAbs (35–37). The combination of small molecule inhibitors of BRAF with anti-EGFR mAbs is the preferred 2^{nd}-line treatment option for this subgroup of patients (38). BRAF V600 mutations segregate in the “immunogenic” consensus molecular subtype-1 CRC that is also characterized by hypermethylation of CpG islands and CTL infiltration in the TME

Author Manuscript Author Manuscript Author Manuscript Author Manuscript

(39). In our single patient with tumor harboring BRAF V600 mutation with available fresh tumor tissue for flow cytometry, there was evidence of high baseline intratumoral T-cell infiltration. It is plausible that the addition of immune checkpoint blockade to EGFR and BRAF inhibition for patients with BRAF V600 mCRC may provide a viable treatment strategy and is currently an active area of clinical investigation (NCT04017650).

Conclusion

The combination of cetuximab plus pembrolizumab was inactive in unselected patients with RASwt CRC, despite showing a significant effectiveness in reprogramming the TME for enhanced CTL accumulation (47% over baseline). A personalized approach incorporating agents targeting other T-cell exhaustion and activation pathways or factors promoting a higher level of CTL influx may be necessary to improve the antitumor efficacy of the EGFR-plus anti-PD-1-based regimens.

Supplementary Material

Refer to Web version on PubMed Central for supplementary material.

Acknowledgements:

This work was partially supported by National Cancer Institute (NCI) grants P30CA016056 and R50CA2111108 (H. Minderman) involving the use of Roswell Park Comprehensive Cancer Center's Flow and Image Cytometry Shared Resource, the Biostatistics and Bioinformatics Shared Resource, and the Pathology Network Shared Resource. This study was presented in part in the American Society of Clinical Oncology 2020 Annual Meeting, the European Society of Medical Oncology 2020 World Congress on Gastrointestinal Cancer, and the European Society of Medical Oncology 2020 Immuno-Oncology Congress.

Funding:

Merck Sharp & Dohme Corp., a subsidiary of Merck & Co., Inc., Kenilworth, NJ, USA provided drug and financial support for the study.

References:

1. Siegel RL, Miller KD, Jemal A. Cancer statistics, 2019. CA Cancer J Clin 2019;69(1):7–34 doi 10.3322/caac.21551. [PubMed: 30620402]
2. Siegel RL, Miller KD, Fedewa SA, Ahnen DJ, Meester RGS, Barzi A, et al. Colorectal cancer statistics, 2017. CA Cancer J Clin 2017;67(3):177–93 doi 10.3322/caac.21395. [PubMed: 28248415]
3. Modest DP, Ricard I, Heinemann V, Hegewisch-Becker S, Schmiegel W, Porschen R, et al. Outcome according to KRAS-, NRAS- and BRAF-mutation as well as KRAS mutation variants: pooled analysis of five randomized trials in metastatic colorectal cancer by the AIO colorectal cancer study group. Ann Oncol 2016;27(9):1746–53 doi 10.1093/annonc/mdw261. [PubMed: 27358379]
4. Peeters M, Kafatos G, Taylor A, Gastanaga VM, Oliner KS, Hechmati G, et al. Prevalence of RAS mutations and individual variation patterns among patients with metastatic colorectal cancer: A pooled analysis of randomised controlled trials. Eur J Cancer 2015;51(13):1704–13 doi 10.1016/j.ejca.2015.05.017. [PubMed: 26049686]
5. Piton N, Lonchamp E, Nowak F, Sabourin JC, group K. Real-Life Distribution of KRAS and NRAS Mutations in Metastatic Colorectal Carcinoma from French Routine Genotyping. Cancer Epidemiol Biomarkers Prev 2015;24(9):1416–8 doi 10.1158/1055-9965.EPI-15-0059. [PubMed: 26189770]

Author Manuscript Author Manuscript Author Manuscript Author Manuscript

6. Douillard JY, Oliner KS, Siena S, Tabernero J, Burkes R, Barugel M, et al. Panitumumab-FOLFOX4 treatment and RAS mutations in colorectal cancer. N Engl J Med 2013;369(11):1023–34 doi 10.1056/NEJMoa1305275. [PubMed: 24024839]
7. Van Cutsem E, Lenz HJ, Kohne CH, Heinemann V, Tejpar S, Melezinek I, et al. Fluorouracil, leucovorin, and irinotecan plus cetuximab treatment and RAS mutations in colorectal cancer. J Clin Oncol 2015;33(7):692–700 doi 10.1200/JCO.2014.59.4812. [PubMed: 25605843]
8. Van Cutsem E, Kohne CH, Hitre E, Zaluski J, Chang Chien CR, Makhson A, et al. Cetuximab and chemotherapy as initial treatment for metastatic colorectal cancer. N Engl J Med 2009;360(14):1408–17 doi 10.1056/NEJMoa0805019. [PubMed: 19339720]
9. Karapetis CS, Khambata-Ford S, Jonker DJ, O'Callaghan CJ, Tu D, Tebbutt NC, et al. K-ras mutations and benefit from cetuximab in advanced colorectal cancer. N Engl J Med 2008;359(17):1757–65 doi 10.1056/NEJMoa0804385. [PubMed: 18946061]
10. Benson AB, Venook AP, Al-Hawary MM, Arain MA, Chen YJ, Ciombor KK, et al. NCCN Guidelines Insights: Rectal Cancer, Version 6.2020. J Natl Compr Canc Netw 2020;18(7):806–15 doi 10.6004/jnccn.2020.0032. [PubMed: 32634771]
11. Zhao B, Wang L, Qiu H, Zhang M, Sun L, Peng P, et al. Mechanisms of resistance to anti-EGFR therapy in colorectal cancer. Oncotarget 2017;8(3):3980–4000 doi 10.18632/oncotarget.14012. [PubMed: 28002810]
12. Weiner GJ. Monoclonal antibody mechanisms of action in cancer. Immunol Res 2007;39(1–3):271–8 doi 10.1007/s12026-007-0073-4. [PubMed: 17917071]
13. Seo Y, Ishii Y, Ochiai H, Fukuda K, Akimoto S, Hayashida T, et al. Cetuximab-mediated ADCC activity is correlated with the cell surface expression level of EGFR but not with the KRAS/BRAF mutational status in colorectal cancer. Oncol Rep 2014;31(5):2115–22 doi 10.3892/or.2014.3077. [PubMed: 24626880]
14. Van den Eynde M, Mlecnik B, Bindea G, Fredriksen T, Church SE, Lafontaine L, et al. The Link between the Multiverse of Immune Microenvironments in Metastases and the Survival of Colorectal Cancer Patients. Cancer Cell 2018;34(6):1012–26 e3 doi 10.1016/j.ccell.2018.11.003. [PubMed: 30537506]
15. Concha-Benavente F, Kansy B, Moskovitz J, Moy J, Chandran U, Ferris RL. PD-L1 Mediates Dysfunction in Activated PD-1(+) NK Cells in Head and Neck Cancer Patients. Cancer Immunol Res 2018;6(12):1548–60 doi 10.1158/2326-6066.CIR-18-0062. [PubMed: 30282672]
16. Trivedi S, Srivastava RM, Concha-Benavente F, Ferrone S, Garcia-Bates TM, Li J, et al. Anti-EGFR Targeted Monoclonal Antibody Isotype Influences Antitumor Cellular Immunity in Head and Neck Cancer Patients. Clin Cancer Res 2016;22(21):5229–37 doi 10.1158/1078-0432.CCR-15-2971. [PubMed: 27217441]
17. Woolston A, Khan K, Spain G, Barber LJ, Griffiths B, Gonzalez-Exposito R, et al. Genomic and Transcriptomic Determinants of Therapy Resistance and Immune Landscape Evolution during Anti-EGFR Treatment in Colorectal Cancer. Cancer Cell 2019;36(1):35–50 e9 doi 10.1016/j.ccell.2019.05.013. [PubMed: 31287991]
18. Liu L, Mayes PA, Eastman S, Shi H, Yadavilli S, Zhang T, et al. The BRAF and MEK Inhibitors Dabrafenib and Trametinib: Effects on Immune Function and in Combination with Immunomodulatory Antibodies Targeting PD-1, PD-L1, and CTLA-4. Clin Cancer Res 2015;21(7):1639–51 doi 10.1158/1078-0432.CCR-14-2339. [PubMed: 25589619]
19. Sill MW, Rubinstein L, Litwin S, Yothers G. A method for utilizing co-primary efficacy outcome measures to screen regimens for activity in two-stage Phase II clinical trials. Clin Trials 2012;9(4):385–95 doi 10.1177/1740774512450101. [PubMed: 22811448]
20. Price TJ, Peeters M, Kim TW, Li J, Cascinu S, Ruff P, et al. Panitumumab versus cetuximab in patients with chemotherapy-refractory wild-type KRAS exon 2 metastatic colorectal cancer (ASPECCT): a randomised, multicentre, open-label, non-inferiority phase 3 study. Lancet Oncol 2014;15(6):569–79 doi 10.1016/S1470-2045(14)70118-4. [PubMed: 24739896]
21. Andre T, Shiu KK, Kim TW, Jensen BV, Jensen LH, Punt C, et al. Pembrolizumab in Microsatellite-Instability-High Advanced Colorectal Cancer. N Engl J Med 2020;383(23):2207–18 doi 10.1056/NEJMoa2017699. [PubMed: 33264544]

Author Manuscript Author Manuscript Author Manuscript Author Manuscript

22. Le DT, Kim TW, Van Cutsem E, Geva R, Jager D, Hara H, et al. Phase II Open-Label Study of Pembrolizumab in Treatment-Refractory, Microsatellite Instability-High/Mismatch Repair-Deficient Metastatic Colorectal Cancer: KEYNOTE-164. J Clin Oncol 2020;38(1):11–9 doi 10.1200/JCO.19.02107. [PubMed: 31725351]

23. Martinelli E, Martini G, Troiani T, Pietrantonio F, Avallone A, Normanno N, et al. 397O Avelumab plus cetuximab in pre-treated RAS wild type metastatic colorectal cancer patients as a rechallenge strategy: The phase II CAVE (cetuximab-avelumab) mCRC study. Annals of Oncology 2020;31:S409–S10 doi 10.1016/j.annonc.2020.08.508.

24. Kim TW, Peeters M, Thomas A, Gibbs P, Hool K, Zhang J, et al. Impact of Emergent Circulating Tumor DNA RAS Mutation in Panitumumab-Treated Chemoresistant Metastatic Colorectal Cancer. Clin Cancer Res 2018;24(22):5602–9 doi 10.1158/1078-0432.CCR-17-3377. [PubMed: 29898991]

25. Parseghian CM, Sun R, Napolitano S, Morris VK, Henry J, Willis J, et al. Rarity of acquired mutations (MTs) after first-line therapy with anti-EGFR therapy (EGFRi). Journal of Clinical Oncology 2021;39(15_suppl):3514- doi 10.1200/JCO.2021.39.15_suppl.3514.

26. Pages F, Berger A, Camus M, Sanchez-Cabo F, Costes A, Molidor R, et al. Effector memory T cells, early metastasis, and survival in colorectal cancer. N Engl J Med 2005;353(25):2654–66 doi 10.1056/NEJMoa051424. [PubMed: 16371631]

27. Galon J, Costes A, Sanchez-Cabo F, Kirilovsky A, Mlecnik B, Lagorce-Pages C, et al. Type, density, and location of immune cells within human colorectal tumors predict clinical outcome. Science 2006;313(5795):1960–4 doi 10.1126/science.1129139.

28. Pages F, Kirilovsky A, Mlecnik B, Asslaber M, Tosolini M, Bindea G, et al. In situ cytotoxic and memory T cells predict outcome in patients with early-stage colorectal cancer. J Clin Oncol 2009;27(35):5944–51 doi 10.1200/JCO.2008.19.6147. [PubMed: 19858404]

29. Tumeh PC, Harview CL, Yearley JH, Shintaku IP, Taylor EJ, Robert L, et al. PD-1 blockade induces responses by inhibiting adaptive immune resistance. Nature 2014;515(7528):568–71 doi 10.1038/nature13954. [PubMed: 25428505]

30. Lee M, Loehrer P, Imanirad I, Cohen S, Ciombor K, Moore T, et al. Phase II study of ipilimumab, nivolumab, and panitumumab in patients with KRAS/NRAS/BRAF wild-type (WT) microsatellite stable (MSS) metastatic colorectal cancer (mCRC). 2021; Virtual. American Society of Clinical Oncology.

31. Innocenti F, Ou FS, Qu X, Zemla TJ, Niedzwiecki D, Tam R, et al. Mutational Analysis of Patients With Colorectal Cancer in CALGB/SWOG 80405 Identifies New Roles of Microsatellite Instability and Tumor Mutational Burden for Patient Outcome. J Clin Oncol 2019;37(14):1217–27 doi 10.1200/JCO.18.01798. [PubMed: 30865548]

32. Overman MJ, Lonardi S, Wong KYM, Lenz HJ, Gelsomino F, Aglietta M, et al. Durable Clinical Benefit With Nivolumab Plus Ipilimumab in DNA Mismatch Repair-Deficient/Microsatellite Instability-High Metastatic Colorectal Cancer. J Clin Oncol 2018;36(8):773–9 doi 10.1200/JCO.2017.76.9901. [PubMed: 29355075]

33. Overman MJ, McDermott R, Leach JL, Lonardi S, Lenz HJ, Morse MA, et al. Nivolumab in patients with metastatic DNA mismatch repair-deficient or microsatellite instability-high colorectal cancer (CheckMate 142): an open-label, multicentre, phase 2 study. Lancet Oncol 2017;18(9):1182–91 doi 10.1016/S1470-2045(17)30422-9. [PubMed: 28734759]

34. Shiu K-K, Andre T, Kim TW, Jensen BV, Jensen LH, Punt CJA, et al. KEYNOTE-177: Phase III randomized study of pembrolizumab versus chemotherapy for microsatellite instability-high advanced colorectal cancer. Journal of Clinical Oncology 2021;39(3_suppl):6- doi 10.1200/JCO.2021.39.3_suppl.6.

35. Chu JE, Johnson B, Kugathasan L, Morris VK, Raghav K, Swanson L, et al. Population-based Screening for BRAF (V600E) in Metastatic Colorectal Cancer Reveals Increased Prevalence and Poor Prognosis. Clin Cancer Res 2020;26(17):4599–605 doi 10.1158/1078-0432.CCR-20-1024. [PubMed: 32571791]

36. Seligmann JF, Fisher D, Smith CG, Richman SD, Elliott F, Brown S, et al. Investigating the poor outcomes of BRAF-mutant advanced colorectal cancer: analysis from 2530 patients in randomised clinical trials. Ann Oncol 2017;28(3):562–8 doi 10.1093/annonc/mdw645. [PubMed: 27993800]

Author Manuscript Author Manuscript Author Manuscript Author Manuscript

37. Di Nicolantonio F, Martini M, Molinari F, Sartore-Bianchi A, Arena S, Saletti P, et al. Wild-type BRAF is required for response to panitumumab or cetuximab in metastatic colorectal cancer. J Clin Oncol 2008;26(35):5705–12 doi 10.1200/JCO.2008.18.0786. [PubMed: 19001320]

38. Kopetz S, Grothey A, Yaeger R, Van Cutsem E, Desai J, Yoshino T, et al. Encorafenib, Binimetinib, and Cetuximab in BRAF V600E-Mutated Colorectal Cancer. N Engl J Med 2019;381(17):1632–43 doi 10.1056/NEJMoa1908075. [PubMed: 31566309]

39. Thanki K, Nicholls ME, Gajjar A, Senagore AJ, Qiu S, Szabo C, et al. Consensus Molecular Subtypes of Colorectal Cancer and their Clinical Implications. Int Biol Biomed J 2017;3(3):105–11. [PubMed: 28825047]

Author Manuscript Author Manuscript Author Manuscript Author Manuscript

Statement of translational relevance

Microsatellite stable metastatic colorectal cancer (mCRC) is resistant to PD-1/L1-targeting immune checkpoint blockade. We performed a phase Ib/II study of the combination of cetuximab and pembrolizumab in *RAS* wild-type mCRC, to test the hypothesis that combining PD-1 inhibition with an anti-epidermal growth factor receptor (EGFR) antibody can induce a more favorable immune tumor microenvironment (TME) and overcome PD-1 resistance. We observed that the tested combination did not improve upon historic results, but it did induce favorable changes in the TME, which included the increase in the intratumoral $CD8^+$ T-cells numbers. The infiltrating cells expressed several exhaustion markers, with striking differences between the primary and metastatic tumor sites. Our data indicate that analysis of the primary tumors may not adequately reflect the immunosuppressive status of the metastatic sites. They suggest that the clinical efficacy of anti-EGFR based therapies may require simultaneous targeting of alternative T-cell exhaustion pathways and additional augmentation of innate immunity.

Author Manuscript Author Manuscript Author Manuscript Author Manuscript

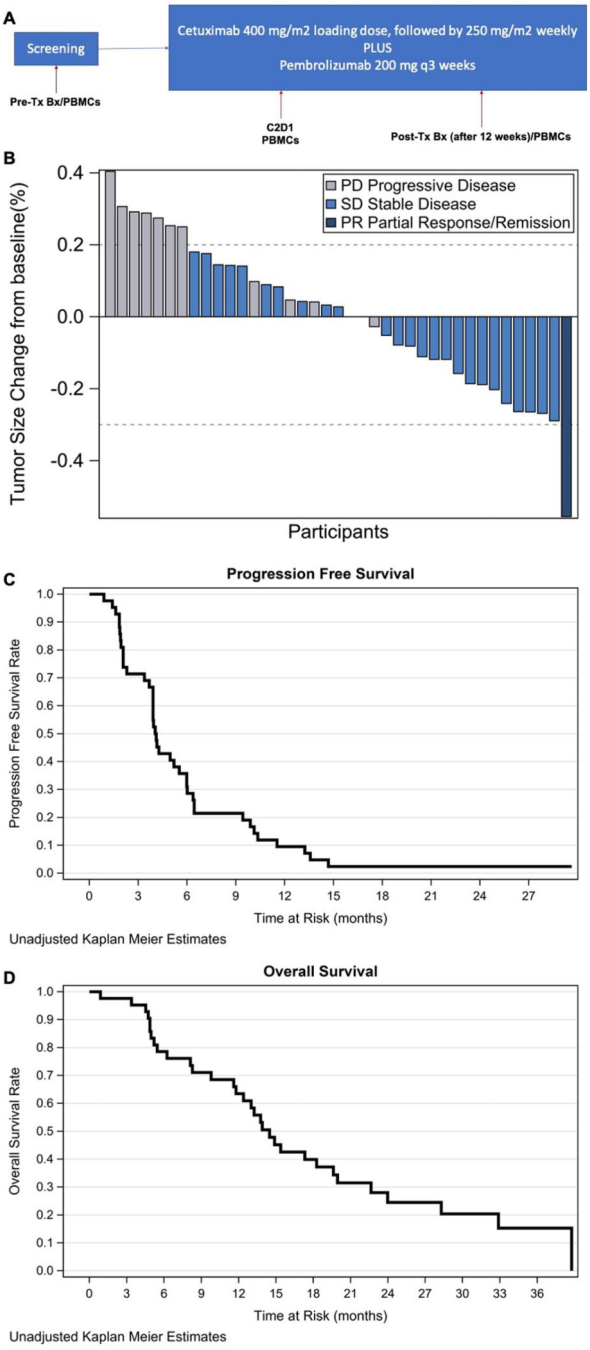

Figure 1.

Study Schema (**A**); overall response rate, waterfall plot (**B**); progression-free (**C**) and overall survival (**D**).

Author Manuscript Author Manuscript Author Manuscript Author Manuscript

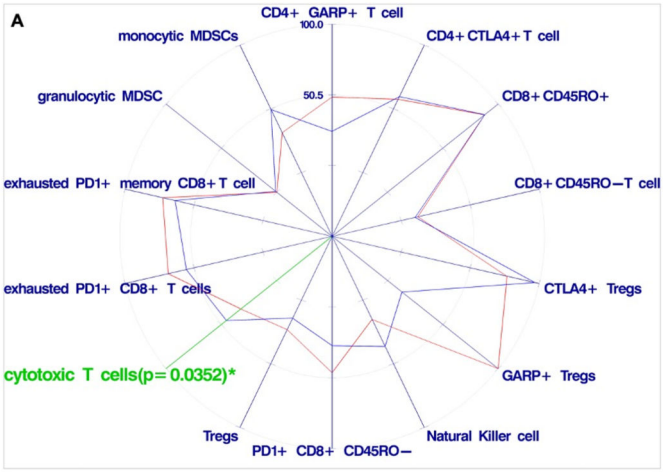

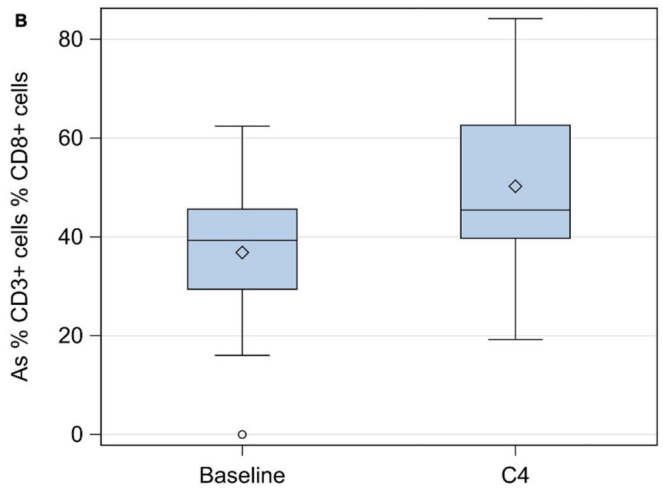

Cell Population	Cycle 1 N	Cycle 1 Median (Min-Max)	Cycle 1 Mean (SD)	Cycle 4 N	Cycle 4 Median (Min-Max)	Cycle 4 Mean (SD)	Percent Change from Cycle 1 N	Percent Change from Cycle 1 Median (Min-Max)	Percent Change from Cycle 1 Mean (SD)	P Value
cytotoxic T-cells	15	33.37 (16.03-46.21)	33.59 (9.54)	15	46.56 (19.22-84.19)	50.64 (17.69)	15	47.05 (-42.33 – 260.07)	64.69 (79.61)	0.0352
exhausted PD1+ CD8+ T-cells	14	69.35 (10.97-100)	62.61 (27.39)	14	56.08 (17.65-95.16)	54.37 (25.04)	14	-23.13 (-82.35 – 382.59)	39.99 (145.41)	0.1796
memory CD8+ T-cells	15	88.6 (22.73-100)	80.71 (21.38)	15	88.24 (36.02-98.39)	82.95 (15.97)	15	1.01 (-60.38 – 275.23)	19.64 (76.37)	0.6072
exhausted PD1+ memory CD8+ T-cells	14	73.59 (28.17-100)	69.04 (22.91)	14	64.11 (21.7-96.72)	58.97 (23.75)	14	-22.95 (-77.78 – 243.34)	8.74 (88.34)	0.1796
CD8+ CD45RO- T-cells	14	13.62 (2.93-77.14)	20.89 (21.32)	14	11.41 (4.56-36.62)	13.74 (9.4)	14	-24.12 (-80.93 – 286.35)	15.69 (106.06)	0.7905
PD1+ CD8+ CD45RO- T-cells	14	47.73 (2.3-100)	46.12 (30.13)	14	28.12 (0-100)	38.95 (29.61)	14	-40.8 (-100 – 1031.89)	177.52 (381.7)	0.7905
Natural Killer cells	15	16.87 (0.18-60.59)	20.84 (17.83)	15	37.05 (6.67-57.06)	32.36 (17.91)	15	113.46 (-86.19 – 4950)	524.72 (1261.06)	0.3018
CD4+ GARP+ T-cells	2	49.41 (16.67-82.14)	49.41 (46.29)	2	25.61 (0-51.21	25.61 (36.21)	2	53.6 (-100 – 207.2)	53.6 (217.22)	1
CD4+ CTLA4+ T-cells	2	58.63 (33.33-83.93)	58.63 (35.78)	2	60.32 (40-80.63)	60.32 (28.73)	2	44.79 (-52.34 – 141.91)	44.79 (137.36)	1
Tregs	2	24.56 (18.75-30.36)	24.56 (8.21)	2	15.97 (12-19.93)	15.97 (5.61)	2	-27.09 (-60.47 – 6.29)	-27.09 (47.21)	1
GARP+ Tregs	2	100 (100-100)	100 (0)	2	14.02 (0-28.04)	14.02 (19.83)	2	-85.98 (-100 – -71.96)	-85.98 (19.83)	0.5
CTLA4+ Tregs	2	77.78 (55.56-100)	77.78 (31.42)	2	97.2 (94.39-100)	97.2 (3.97)	2	34.94 (0 – 69.89)	34.94 (49.42)	1
monocytic MDSCs	2	32.52 (15.04-50)	32.52 (24.72)	2	50 (0-100)	50 (70.71)	2	232.45 (-100 – 564.89)	232.45 (470.15)	1
granulocytic MDSC	1	1.27 (1.27-1.27)	1.27	1	2.33 (2.33-2.33)	2.33	1	83.46 (83.46– 83.46)	83.46	1

Figure 2.

Changes in intratumoral immune cell populations on-treatment, spider plot **(A)** and change in intratumoral cytotoxic T-cell lymphocytes **(B).** (cytotoxic T-cells: % CD3+ cells % CD8+ cells; exhausted PD1+ CD8+ T-cells: % CD3+ cells % PD1+ CD8+ cells: memory CD8+ T-cells: % of CD8+ cells % CD8+ CD45RO+ cells; exhausted PD1+ memory CD8+ T-cells: % of CD8+ cells % PD1+ CD45RO+ cells; CD8+ CD45RO- T-cells: % of CD8+ cells % CD8+ CD45RO- cells; PD1+ CD8+ CD45RO- T-cells: % of CD8+ cells % PD1+ CD45RO- cells; Natural Killer cells: % CD3- cells % CD56+ CD16+ cells; CD4+ GAPR+ T-cells: % of CD3+ cells % CD4+ GARP+ cells; CD4+ CTLA4+ T-cells: % of CD3+ cells % CD4+ CTLA4+ cells; Tregs: % of CD4+ cells % CD25+ FoxP3+ cells; CTLA4+ Tregs: % of CD25+FoxP3+ cells % CTLA4+ Tregs; monocytic MDSCs: % of CD14+ HLADR-

% CD33+ CD11b+ cells; granulocytic MDSCs: % of CD14- HLADR- % CD33+ CD11b+ cells). MDSCs=myeloid-derived suppressor cells.

Author Manuscript Author Manuscript Author Manuscript Author Manuscript

Author Manuscript Author Manuscript Author Manuscript Author Manuscript

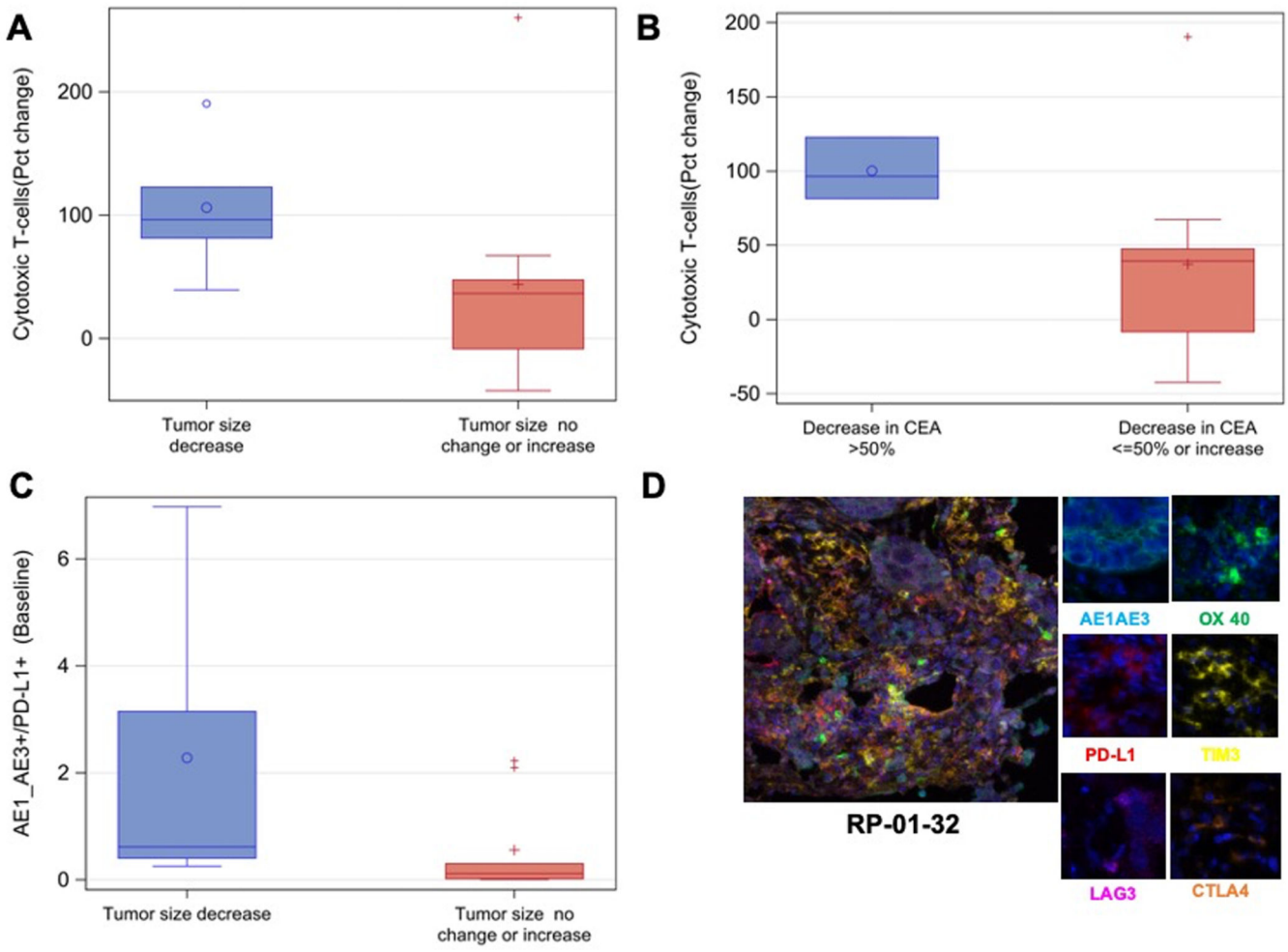

Figure 3.

Intratumoral cytotoxic T-cell lymphocyte changes on treatment by change in tumor size (**A**) and change in CEA (**B**). Higher expression of PD-L1 in tumor cells at baseline correlated with decrease in tumor burden (**C**). Representative multiplexed images from pre-treatment tumor tissue in patient RP-01–32 who attained a partial response (**D**) with composite image (left panel) and individual markers (right panels).

Author Manuscript
Author Manuscript
Author Manuscript
Author Manuscript

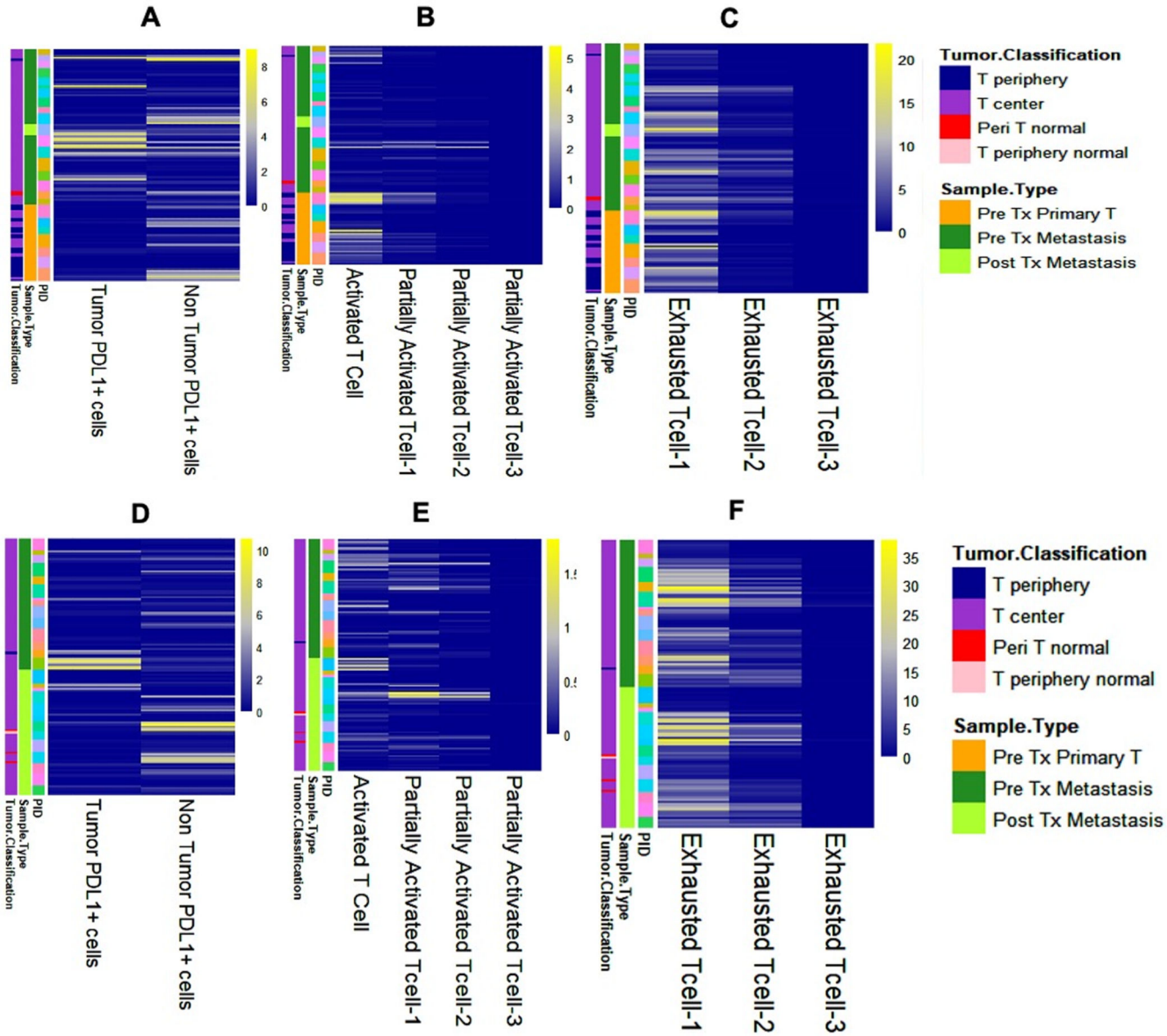

Figure 4.

Heatmap classified based on pre-treatment primary tumor vs. pre-treatment metastasis biopsy (**A-C**) showing number of (**A**) PD-L1 positive tumor cells (AE1_AE3^{+}/PDL1^{+}) and PD-L1 positive non-tumor cells in tumor microenvironment (AE1_AE3^{-}/PDL1^{+}); (**B**) activated T-cell subsets; (**C**) and exhausted T-cell subsets. Heatmap classified based on pre-treatment vs. post-treatment biopsy (**D-F**) showing number of (**D**) PD-L1 positive tumor cells (AE1_AE3^{+}/PDL1^{+}) and PD-L1 positive non-tumor cells in tumor microenvironment (AE1_AE3^{-}/PDL1^{+}); (**E**) activated T-cell subsets; (**F**) exhausted T-cell subsets.

Author Manuscript Author Manuscript Author Manuscript Author Manuscript

A

						Biomarkers (degree of expression)				
RP code	Status	Prior Exposure to Immune Checkpoint Inhibitor	Best Response	Tumor Burden	CEA	OX 40	TIM3	CTLA4	LAG3	PD-L1
RP-01-23	MSI-H/pMMR	No	Stable Disease	26% Decrease	97% Decrease	Low	High	Low	Low	Low
RP-01-06	MSI-H/dMMR	Yes	Stable Disease	3% Increase	No Change	Low	Intermediate	Low	Low	Intermediate
RP-01-04	dMMR	Yes	Stable Disease	3% Increase	9% Decrease	Low	Intermediate	Intermediate	Low	High
RP-01-09	dMMR	No	Progressive Disease	29% Increase	64% Decrease	Low	High	High	Low	High

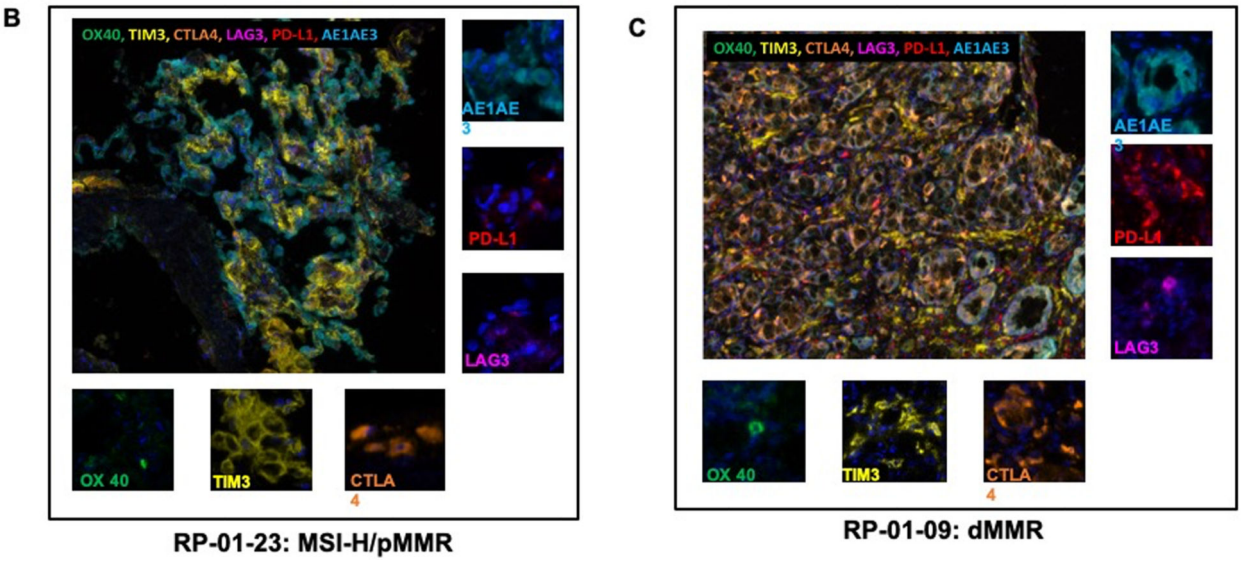

Figure 5.

Patients with microsatellite-instability (MSI-H) or mismatch-repair deficient (dMMR) tumors; summary of outcomes and immune checkpoint expression by multiplex immunofluorescence (**A**), representative multiplexed images from pre-treatment tumor tissue in patient RP-01–23 with near partial response (**B**) and RP-01–09 with progressive disease (**C**) with composite image (large panel) and individual markers (small panels).

Author Manuscript Author Manuscript Author Manuscript Author Manuscript

Table 1.

Baseline Demographics (N=44)

Age (median/range)	64.2 (33.5–79.6)
Gender (N/%)	
Male	30 (68)
Female	14 (32)
Race (N/%)	
Caucasian	42 (95)
African American	2 (5)
Microsatellite Instability (N/%)	
Stable	19 (43)
Low	2 (4.5)
High	2 (4.5)
Unknown	21 (48)
Mismatch Repair (N/%)	
Deficient	3 (7)
Proficient	38 (93)
BRAF (N/%)	
Wild-type	37 (84.1)
Mutant (V600)	2 (4.5)
Unknown	5 (11.4)
Primary Tumor Location (N/%)	
Right	12 (27)
Left	32 (73)
ECOG PS (N/%)	
0	25 (57)
1	19 (43)
Prior Oxaliplatin/FOLFOX (N/%)	
Yes	43 (98)
No	1 (2)
Prior Irinotecan/FOLFIRI (N/%)	
Yes	27 (61)
No	17 (39)
Prior Bevacizumab (N/%)	
Yes	31 (71)
No	13 (29)
Prior cetuximab/panitumumab (N/%)	

Author Manuscript Author Manuscript Author Manuscript Author Manuscript

Yes	3 (7)
No	41 (93)
Prior fluoropyrimidine (N/%)	44 (100)
Prior Surgery (N/%)	
Yes	39 (89)
No	5 (11)
Prior Radiotherapy (N/%)	
Yes	16 (36)
No	28 (64)
Number of Metastatic Sites (median/range)	2 (1–3)
Treatment starting time since diagnosis (Months)	
New Treatment During Follow-up (N/%)	
Yes	10 (23)
No	34 (77)